Suchański et al. EURASIP Journal on Wireless Communications and Networking (2020) 2020:189
https://doi.org/10.1186/s13638-020-01803-4

EURASIP Journal on Wireless Communications and Networking

RESEARCH Open Access

Radio environment maps for military cognitive networks: density of small-scale sensor network vs. map quality

Marek Suchański, Paweł Kaniewski, Janusz Romanik, Edward Golan and Krzysztof Zubel*

* Correspondence: k.zubel@wil.waw.pl
Radiocommunications & Electronic Warfare Division, Military Communication Institute, Warszawska 22A, 05-130 Zegrze Poludniowe, Poland

Abstract

In this paper, we present the dependency between density of a sensor network and map quality in the radio environment map (REM) concept. The architecture of REM supporting military communications systems is described. The map construction techniques based on spatial statistics and transmitter location determination are presented. The problem of REM quality and relevant metrics are discussed. The results of field tests for UHF range with a different number of sensors are shown. Exemplary REM maps with different interpolation algorithms are presented. Finally, the problem of density of a sensor network versus REM map quality is analyzed.

Keywords: Cognitive radio, Radio environment map, Spectrum monitoring, Density of sensor network, Deployment of sensors

1 Introduction

In recent years in many fields of technology, there has been a growing trend towards creating intelligent solutions that autonomously make decisions about their actions. This trend can also be noticed in wireless communications. It is worth mentioning here such solutions as self-organizing networks [1, 2], disruption-tolerant networks [3], dynamic spectrum management [4, 5], and cognitive radio [6]. In military communications, new technical solutions are adopted with great caution as they are used in very specific conditions and have to be extremely reliable. Military wireless networks need to be immune to deliberate interference and to remain operational even in the case of systematic destruction of telecommunication infrastructure. Since one of the main challenges at the tactical level is the high maneuverability of troops, specific technical answers are required. A promising solution to the problem is MANET (mobile ad-hoc network). The main advantage of MANET is their ability to self-organize in the environment where users frequently and unpredictably change their location. Moreover, in MANET, all radios play the role of user terminals and relay nodes.

The problem of efficient frequency management in common operations has been noticed by NATO Science and Technology Organization.

As a consequence, the information systems technology (IST) panel has established an exploratory team and then a research task group (RTG) whose tasks include, inter alia, checking potential benefits resulting from the implementation of the radio environment map (REM) concept.

The aim of the IST-146 RTG-069 group is to work out a concept of REM enabling their users to obtain the spectrum operational picture and to minimize the level of interferences between wireless systems of coalition forces. One of the main goals of the research group is to define the architecture of the system and to specify interfaces to other systems in the area of frequency management.

Prior to the establishment of RTG-069, some conceptual work was carried out to find the most appropriate way of introducing cognitive radios to NATO communication systems. The task had a high degree of complexity because it required modification of the existing system without disrupting its operation or limiting its functionality even temporarily. There were two RTGs set up to solve the problem. The solutions proposed by the first group were not accepted by the appropriate NATO Capability Team due to concerns about a temporary spectral resource deficit. The other team—NATO IST-104 RTG-050—divided the path to the goal into two main phases in which small steps (the so-called "baby steps") were distinguished. REM implementation is one of such baby steps needed to make significant progress towards a coordinated spectrum management system in NATO [4].

1.1 REM architecture

In general, REM is considered to be a database which stores comprehensive and up-to-date information on the radio spectrum. It is assumed that this information is composed of geographical features, available services, spectral regulations, positions and activities of radios, and policies adopted by the user and/or service providers, as well as knowledge from the past [7].

The simplified architecture of REM excerpted from [8, 9] and adapted to military applications is presented in Fig. 1. REM architecture comprises the following modules: REM Manager, REM storage and data collection, REM Acquisition, sensors, and GUI. REM Manager processes the data and controls the REM database in terms of measurement configuration, e.g., monitoring subranges, measurement mode (continuous or on

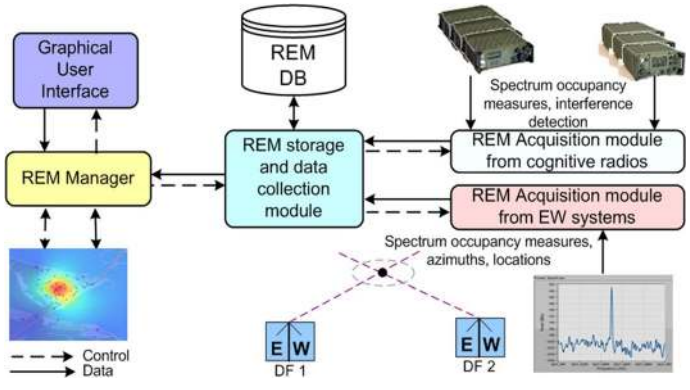

Fig. 1 REM architecture to support tactical operation

request), and active sensors. REM storage and collection module is an interface between the database, REM acquisition modules, and REM Manager. REM acquisition modules are interfaces to various systems of sensors.

In the literature [10], sensors are generally named MCDs (measurement capable devices). MCDs are controlled through REM Acquisition modules and they monitor spectrum. In civilian applications, the function of MCDs can be performed by various devices with measurement capability, such as simple mobile phones, smart phones, and notebooks.

When military systems are considered, spectrum measurements can be taken by dedicated receivers, cognitive radios, electronic warfare (EW) systems, or intelligence, surveillance, reconnaissance (ISR) systems [11, 12]. It is worth noting that sensors are strictly connected to specific military platforms, e.g., trucks. As a consequence, the position of the sensor results from the operational needs for the platform and thus cannot be changed freely, e.g., to get better distribution of sensors. For this reason the possibility of deployment of sensors in tactical environment may be seriously reduced.

1.2 Related works

In the literature on the topic, the spectrum sampling method for REM has not been thoroughly researched. Although the process of collecting the results of measurements to construct REM can be carried out by dedicated sensors with fixed positions and mobile devices (e.g., cognitive radios), the resources of mobile devices are more limited since they have to use their battery efficiently [13]. Therefore, the problem of how the density of sensor network affects the quality of the REM must be addressed.

In [14], the authors performed an experiment in real conditions whose aim was to determine the position of a transmitter operating at 800 MHz frequency with the application of the indirect method. The transmitter was placed inside a grid consisting of 49 nodes in a 7 × 7 arrangement, spaced 5 m apart. The results of measurements and calculations showed that at least 20 randomly selected sensors are necessary in order to determine the position of the transmitter with sufficient accuracy. In such a case, the error of determining the position of the transmitter was about 1.5 m. When the results of measurements from 46 sensors were taken into account, the error of position determining decreased to about 1 m, which is 20% of the distance between the sensors in the grid.

In [15], the authors discussed a method of searching for white spaces in UHF band (470–900 MHz) which could be used for cognitive radio (CR). Some field tests were performed with 100 measurement units deployed in the area of 5 km^2 and distributed in two ways: regular lattice (Cartesian) and pseudo-random. The authors noticed the relation between the number of measuring sensors and the required terrain resolution of the REM map being created and the number of CR users per square kilometer.

In [16], the authors presented three methods of creating REM: the path loss-based method, the Kriging-based method, and their own method. To compare the efficiency of the proposed methods, a series of simulations were performed for a scenario with (a) one transmitting node, (b) 81 sensing nodes, and (c) 8 validating nodes which do not overlap with the 81 sensors. All the nodes were deployed in the area of 70 m by 70 m. To assess the quality of the created REMs the root mean square error (RMSE) was calculated for the 8 validating nodes.

The accuracy of determining the location of the transmitter in meters was used as a measure of the quality of REM maps in [17]. The environment considered in the research work was a simulated urban macro-cell square area of 1 km^2. In this area, one transmitter and up to 20 measuring sensors were placed randomly. REM maps were developed using two indirect methods: one based on received signal strength (RSS) and the other one based on received signal strength difference (RSSD). The authors confirmed a noticeable improvement in the quality of REM maps when the number of sensors is increased to 14–20 per square kilometer.

The paper [18] presented the results of simulation tests for 5G technology in the field of the so-called context-aware resource allocation. These tests consisted of determining at each point of the macro-cell the level of the electromagnetic field originating from the base station. The base station was placed in the center of a 190 by 190 m macro-cell. In this area, 200 sensors were randomly placed, out of which a maximum of 20 sensors were selected to form clusters for the purpose of interpolation of the radio signal level at each point of the macro-cell. In this way, an REM map was created for the entire macro-cell area. Since all the sensors were battery-powered, the factor optimizing the lifetime of the sensor network was the intensity of the use of the sensors involved in the measurement. The algorithm for selecting sensors for the cluster was an own solution proposed by the authors of the article. The resulting REM map obtained using this method was delivered to the 5G base station as a context that allows selection of the operating parameters of this station for communication with end devices located anywhere in the macro-cell.

In the article [19], the authors presented a method of measuring radio emissions from DVB-T digital terrestrial transmitters. The measurements were carried out in the center of Poznan (Poland) using a mobile sensor built-in on a passenger car traveling along a fixed route through the city center. The measurements were carried out in typical everyday traffic conditions. Measurement samples were collected at constant intervals, while the speed of the measurement vehicle was dependent on the indications of traffic lights at each intersection. Therefore, the number of measurement samples per route points was different. The length of the measuring route was 8 km and it ran through various areas from housing estates, through compact and low buildings of the Old Town Square, to recreational areas located between the Warta River and Malta Lake. The measurements showed that when using local REM maps it is possible to start low-power base stations using the so-called TV white spaces.

In the literature on the topic, both kinds of methods of map creation are analyzed, that is the direct methods and the indirect methods, but it seems that the indirect methods prevail. In our paper, however, we deal with the REM maps created with the use of a few selected direct methods, which are described in the next chapter.

In order to assess the quality of REMs with different numbers of sensors used for the interpolation in our research work, we used data obtained from real field tests and RMSE as a quality metric, similarly to [16]. The size of the area (approx. 4 km^2) was similar to the one presented in [15]. Although the number of sensors was smaller than the number typically analyzed, it was comparable to [14, 17].

For the interpolation process, similarly to the method described in [18], we used a limited number of sensors being the selected subset of all the sensors deployed within the geographical area.

Like in the scenario presented in [19], in order to get the measurement data, we used a mobile sensor installed on a military truck.

It is worth noting that our research differs from the research described in the literature not only in terms of the number of sensors used but also in the manner of their distribution. These differences stem from the fact that the scenarios which we considered reflect networks used during small tactical operations, i.e., dozens of sensors operating in the area of several square kilometers. In military operations, the role of sensors is played by cognitive radio stations and therefore the tactical situation determines their distribution. The scenarios presented in the literature usually assume that there are hundreds of sensors spaced quite regularly or arranged in a controlled manner.

1.3 Contributions of the paper

In the paper, we discuss the concept of REM and the problem of the number of sensors from the point of view of tactical operation. We also present exemplary maps created using different interpolation methods and analyze how the number of sensors affects the quality of the maps. Additionally, we focus on the possibility of localization of the TX antenna in reference to selected interpolation techniques.

The rest of the paper is organized as follows: methods and materials (Section 2), results and discussion (Section 3), and conclusions (Section 4).

2 Methods and materials

2.1 Measurement environment and setup

In order to investigate the impact of the number of sensors on the REM quality, several tests were conducted for UHF frequency band. First, measurements were taken in a real environment with 39 sensors to get input data and then, exemplary maps were created using different construction techniques, namely nearest neighbor, inverse distance weighting (IDW), and Kriging. After that, the analysis of calculated root mean square error (RMSE) for various numbers of sensors was made.

Some preliminary tests were conducted with the aim to calibrate the TX and RX sites and to select an area with strong and stable received signal suitable for the final tests. Data collection was arranged in such a way that all measurements were taken on the same day within the period of a few hours to get as similar conditions for all the measurements as possible. The software controlling the RX site measured the received signal ten times and recorded the average value.

To assess the quality of the maps created with the selected interpolation techniques, we analyzed the results for three scenarios with a different number of sensors each, see Table 1. For each scenario, we randomly selected a certain number of sensors for the interpolation process. The remaining sensors were treated as control sensors. As a consequence, for each scenario, we got a different number of control sensors. When there were 13 measuring sensors (Scenario_13), the remaining 26 sensors were used as control sensors. When the number of measuring sensors was set to 20, consequently, there were 19 control sensors. For the scenario with 26 measuring sensors, the remaining 13 sensors served as control sensors. Each of the three scenarios consisted of two tests (Test_a and Test_b), which were performed with a different (random) deployment of

Table 1 Scenarios and tests for RMSE analysis

Number of measurement sensors per number of control sensors	The name of scenario	The name of test
13/26	Scenario_13	Test_13a
		Test_13b
20/19	Scenario_20	Test_20a
		Test_20b
26/13	Scenario_26	Test_26a
		Test_26b

sensors. It is worth noting that the sensors were arranged irregularly due to the fact that the measurements were taken in a real environment.

The initial distribution of 39 sensors is shown in Fig. 2. For the interpolation process, the sensors selected in each test were chosen in a random process, see Table 2. For the control sensors, in each test, the differences between the measured and the interpolated signal level were compared and used to calculate the RMSE. Finally, average values of the RMSE were calculated for each scenario.

In order to perform measurements in a real environment, we established a test set composed of a transmitting part and a receiving part.

The transmitting part of the system consisted of a signal generator connected to a controlling computer, an amplifier and an antenna mounted on the roof of a building at the height of 8 m.

The receiving part consisted of an antenna installed on a vehicle, a radio receiver, and a computer controlling the receiving operation and recording the results of the

Fig. 2 Deployment of the sensors and position of the TX antenna

Table 2 Sensors selected in each test for the interpolation process

Test_13a	Test_13b	Test_20a	Test_20b	Test_26a	Test_26b
P2	P2	P1	P2	P1	P2
P3	P3	P3	P3	P2	P5
P5	P7	P4	P5	P3	P6
P10	P10	P7	P8	P4	P7
P12	P12	P9	P10	P6	P8
P19	P15	P11	P12	P7	P9
P21	P19	P12	P15	P9	P10
P23	P21	P14	P16	P10	P12
P29	P23	P16	P19	P11	P13
P32	P29	P17	P21	P12	P14
P33	P32	P19	P24	P14	P15
P35	P33	P22	P26	P16	P17
P37	P37	P25	P28	P17	P18
-	-	P26	P29	P19	P20
-	-	P27	P31	P21	P22
-	-	P32	P32	P22	P23
-	-	P34	P33	P24	P25
-	-	P36	P35	P25	P26
-	-	P38	P37	P27	P28
-	-	P39	P38	P29	P30
-	-	-	-	P30	P31
-	-	-	-	P32	P33
-	-	-	-	P34	P34
-	-	-	-	P36	P35
-	-	-	-	P38	P37
-	-	-	-	P39	P38

measurements. The antenna was installed at the height of 3 m. The vehicle was moving within a preliminarily selected area, Fig. 2. The configuration of the test set is presented in Table 3.

The measurements were taken in the area of Zegrze Lake in Central Poland (the area of approximately 4 km^2 presented in Fig. 2). The test area was diverse in terms of coverage (partly an open meadow neighboring a forest and partly an urbanized area with medium-sized and high buildings). There were NLOS (non-line-of-sight) conditions for the following sensors:

- P6–P8, P10, P11, P24, P25, P27, and P29—the average height of the forest separating sensors is about 35 m.
- P2, P18–P22, P30, and P31—the approximate height of the buildings separating sensors is between 12 and 15 m.
- P1, P3–P5, P9, P12–P17, P23, P26, P28, P35, and P36—the approximate height of the buildings and single trees separating sensors ranges from 8 up to 10 m.

Table 3 Test set configuration

Test frequency (UHF band)	1997 MHz
Output power	10 W
Modulation type	CW
Measured param.	Averaged RSS
No. of averages	10
Antenna type (TX/RX site)	Omnidirectional

For the sensors P32–P34 and P37–P39, LOS (line-of-sight) conditions could be observed.

2.2 Measurement results

The measurement results collected for all the 39 points (sensors) are presented in Table 4. The geographical coordinates and sensors' ID correspond to the deployment of the sensors shown in Fig. 2. The average levels of measured signals are expressed in dBm. The variance was about $3\,\mathrm{dB}^2$ for most of the sensors and reached $7.4\,\mathrm{dB}^2$ in the worst case.

2.3 Map construction techniques

In the literature on the topic, there is a description of three main categories of the REM construction techniques, namely *direct*, *indirect*, and *hybrid* [10, 20]. *Direct* methods, also called *spatial statistics-based methods*, are based on the interpolation of the measured data, while *indirect* methods, also known as *transmitter location-based methods*, apply transmitter location and propagation model to obtain the estimated value, Fig 3. *Hybrid* methods combine both manners.

Spatial statistics-based methods use measurement data taken at certain locations. In the case of REM, the measurement is done at the location of the sensors. It is understandable that placing sensors in all required locations is impractical or simply impossible. For this reason, samples from sensors are used as an input for the estimation process that can employ different kinds of techniques.

When REM is considered, the most promising estimation techniques described in the literature are as follows: nearest neighbor (NN), inverse distance weighting (IDW), and Kriging.

The nearest neighbor method is considered to be one of the simplest methods but it offers little accuracy. NN uses Thiessen (or Voronoi) polygons, which are defined by boundaries with equal distances from the points at which measurements were taken. A specific feature of these polygons is the fact that their boundaries are exactly in the middle of the distance between neighboring points.

IDW method is based on the assumption that the signal value P_1 at a given point (x_1, y_1) is much more dependent on the values in the nearest measurement points than on samples taken at distant points. To interpolate the signal value, the IDW uses weighting factors w_i that are inversely proportional to the distance between the given point (x_1, y_1) and the sampling point (x_i, y_i) and raised to the power p. The power p determines how the weighting factors decrease with the distance. If the power p value is set high,

Table 4 Results of measurements

Sensor ID	Latitude	Longitude	Signal level [dBm]
P1	52.45390833	21.00674833	− 72.087
P2	52.45294833	21.00970667	− 94.82
P3	52.45216833	21.00846667	− 77.935
P4	52.4508	21.00642	− 88.057
P5	52.45008167	21.00486167	− 88.625
P6	52.450235	21.003245	− 100.77
P7	52.450935	21.00240833	− 96.821
P8	52.45229167	21.00102	− 93.106
P9	52.44887833	21.00480167	− 96.386
P10	52.44482	20.99988167	− 100.76
P11	52.44415833	20.996475	− 100.73
P12	52.44123	21.01492667	− 102.20
P13	52.44405	21.005135	− 100.97
P14	52.44716167	21.004205	− 96.756
P15	52.448385	21.00562833	− 100.3
P16	52.44962333	21.00723	− 85.686
P17	52.45104	21.0091	− 99.576
P18	52.45305333	21.01176333	− 90.147
P19	52.453865	21.01358833	− 95.426
P20	52.45606667	21.011425	− 97.96
P21	52.45544333	21.01000833	− 101.29
P22	52.456415	21.00738333	− 104.27
P23	52.456365	21.00446	− 87.69
P24	52.45536333	21.00042833	− 93.598
P25	52.453935	20.99994167	− 100.31
P26	52.45470667	21.003115	− 86.089
P27	52.45770167	21.00118167	− 98.633
P28	52.45799667	21.00278667	− 97.605
P29	52.45889	20.99992167	− 98.734
P30	52.45421	21.01242667	− 100.80
P31	52.45346	21.01116	− 101.11
P32	52.45427333	21.004795	− 69.633
P33	52.45342833	21.00353667	− 67.873
P34	52.451185	21.00557333	− 70.594
P35	52.45081667	21.00459667	− 87.471
P36	52.45181167	21.004345	− 80.195
P37	52.45222167	21.005275	− 59.779
P38	52.45284167	21.00700333	− 71.768
P39	52.45311167	21.005705	− 64.569

the points which are nearby have stronger impact. When the power p value is set at zero, regardless of the distance, the weighting factors remain at the same level.

The general formula for the IDW method is [13]:

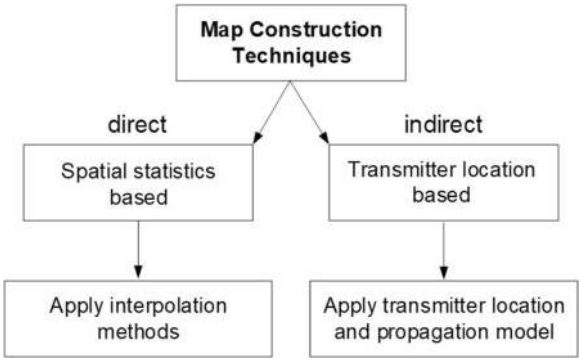

Fig. 3 REM construction methods

$$\hat{V}(x_0) = \sum_{i=1}^{N} w_i(x_0) \cdot V(x_i) \tag{1}$$

where $\hat{V}(x_0)$ is the predicted signal level for point x_0, N is the number of points for which the signal level was measured, w_i is the weighing factor, and $V(x_i)$ is the signal level measured at location x_i.

The formula to determine the weights for the IDW method is given below [13].

$$w_i = \frac{\left(\frac{1}{h_i}\right)^p}{\sum_{i=1}^{n}\left(\frac{1}{h_i}\right)^p} \tag{2}$$

where h_i is the distance between point x_i and point x_0, and p is the power (usually p is set to 1 or 2).

In the rest of the paper, we use the following notation for IDW method: IDW px where x is the power.

Kriging is one of the geostatic methods of interpolation. Like IDW, Kriging uses weighting factors but they are determined on the basis of the semivariogram. This semivariogram is based on the distance between measurement points and the variation between measurements of signal levels as a function of the distance.

Semivariance is calculated according to the formula [21]:

$$\overline{\gamma}(h) = \frac{1}{2|N(h)|}\sum_{N(h)}\left(\left(V(x_1) - V\left(x_j\right)\right)\right)^2 \tag{3}$$

where $h = x_i - x_j$ is the distance between points x_i and x_j, $V(x_i)$ and $V(x_j)$ are the levels of the signal measured at points x_i and x_j, and N is the number of points where the signal levels were measured.

The general formula for Kriging is [21]:

$$\hat{V}(x_0)|_N = \sum_{i=1}^{N} w_{i|N}(x_0) \cdot V(x_i) \tag{4}$$

where $\hat{V}(x_0)$ is the predicted signal level for point x_0.

Kriging is considered to be the most accurate, though quite a complex method of interpolation.

In the literature on REM, the use of Kriging in combination with another method of the signal level determining or the modification of Kriging is proposed [22, 23]. A more detailed description of the estimation techniques mentioned above is presented in [11].

Computational complexity of the different interpolation methods was widely discussed in [7]. Asymptotic computational complexity and calculated complexity for scenarios with 13, 20, and 26 sensors were compared in Table 5.

where M is the number of locations where signal levels are to be estimated; N is the number of sensors; $M, N \rightarrow \infty$; and $M > N$.

Computational complexity with 20 sensors for Kriging is more than 300 times as high as for NN method with the same number of sensors.

The value of the M parameter depends on the required spatial resolution and the size of the REM map. In this case, the digital terrain elevation data (DTED) maps, for which the spatial resolution ranges from 900 m (DTED level 0) to 30 m (DTED level 2), can be used as a reference. For the size of the area analyzed in this paper (4 km^2) with a spatial resolution the same as for DTED level 2, we obtain about 4500 estimated REM locations.

For the assumed area and spatial resolution, the difference in computational complexity for individual interpolation methods did not have a significant impact on the duration of calculations.

The problem of computational complexity and its impact on the selection of an interpolation method may be noticeable for larger areas and for higher spatial resolutions of REMs.

2.4 Exemplary maps

Some exemplary maps for the scenario with 26 sensors constructed with the four interpolation techniques are presented in Fig. 4. The signal level is expressed in dBm and represented by colors (see the legend at the bottom of Fig. 4).

The NN method (Fig. 4, nearest neighbor) creates polygons around each sensor. The size and the shape of the polygons depend on the number and the arrangement of neighboring sensors. Within each polygon the signal strength takes the value measured by the sensor. For this reason, the signal strength changes suddenly at the edges of polygons, e.g., between the orange polygon close to the center and the dark blue one to its right.

The IDW method (Fig. 4, IDW p1 and IDW p3) generates smoother maps when compared to NN. However, the bull's-eye effect occurs and the size of eyes depends on

Table 5 Computational complexity

Method	Asymptotic complexity	Complexity for N sensors		
		$N = 13$	$N = 20$	$N = 26$
NN	$O(M \log N)$	$O(M1,1)$	$O(M1,3)$	$O(M1,4)$
IDW	$O(MN)$	$O(M13)$	$O(M20)$	$O(M26)$
Kriging	$O(MN^2)$	$O(M169)$	$O(M400)$	$O(M676)$

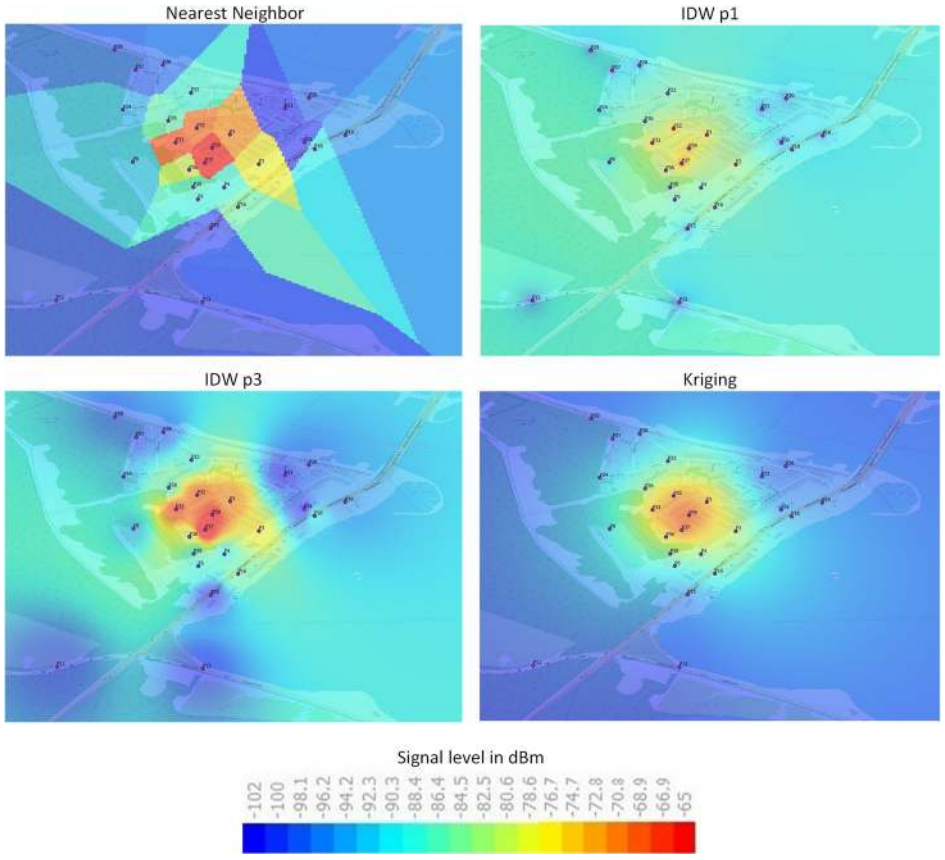

Fig. 4 Comparison of measurement-based maps for selected interpolation techniques

the power p used in the interpolation process. The estimation of the signal strength is quite accurate if the power p is set at 3 or higher and the sensors are deployed densely.

When Kriging is applied (Fig. 4, Kriging), the signal value changes smoothly within the whole area. Kriging seems to be the method which is least sensitive to the deployment of the sensors. Neither bull's-eye effects nor rapid changes in the signal value are observed even if the sensors are deployed sparsely or irregularly.

In the presented scenario, the position of the TX antenna can be determined with the accuracy of approximately the following:

- 350 m for IDW p1
- 300 m for NN
- 250 m for IDW p3
- 150 m for Kriging

Some exemplary maps for NN interpolation technique for different numbers of sensors are presented in Fig. 5. The lowest signal level is represented by the dark blue color, while the highest level by the red color. The comparison of the maps reveals quite clearly visible differences. In the map with 13 sensors (Fig. 5, 13 sensors), the polygons are relatively large and some of them are of irregular shape. When the number of sensors increases, the polygons become smaller with more compact shape (Fig.

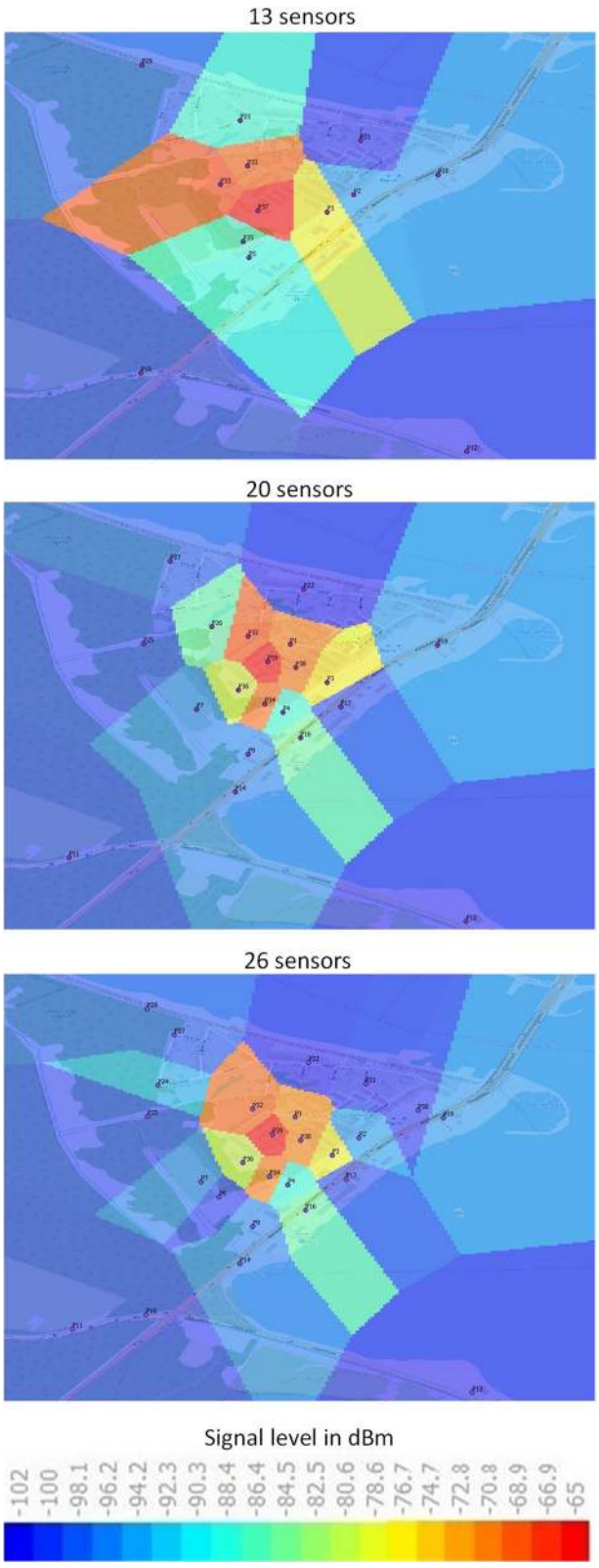

Fig. 5 Maps constructed for NN interpolation technique. Maps were created for various numbers of sensors

5, 20 sensors and 26 sensors). Moreover, in that case, there are more polygons representing medium level of the emission and they surround the polygons with the highest level. As a result, the map looks more regular. If the number of sensors is very low (Fig. 5, 13 sensors), there are a few polygons that represent medium level of the radio signal. In such a situation, an unnatural effect occurs, namely the polygons exemplifying high signal levels are neighboring with the low-level ones.

Some exemplary maps for IDW p3 interpolation technique for various numbers of sensors are shown in Fig. 6. The lowest signal level is represented by the dark blue color while the highest level by the red color. The map presented in Fig. 6, 13 sensors, seems to be unnatural since there is quite an extensive yellow and green area representing the medium signal strength, even for those regions that are distant from the TX antenna. The bull's-eye effect with the dark blue color is present in a few places only. The general conclusion is that there are too few sensors and that they are deployed too sparsely.

The map shown in Fig. 6, 20 sensors, was created with the input data from 20 sensors. There is more of bull's-eye effect with the dark blue color surrounding the central part of the map where the source of emission was located. However, there are quite many regions further away from the TX antenna which are marked with yellow and green color.

The map presented in Fig. 6, 26 sensors, looks more natural when compared to the maps shown in Fig. 6, 13 sensors and 20 sensors. Since the sensors are arranged much more densely, the red-orange center of the map is quite regularly enclosed by the dark blue color of the bull's-eye effect. Moreover, the increased number of sensors caused better reflection of the signal level for those areas that are distant from the TX antenna (medium low signal level represented by the blue color).

Some exemplary maps for Kriging interpolation technique for various density of sensor network are shown in Fig. 7. The dark blue color represents the lowest signal level while the red color the highest. As the number of sensors increases, the map seems to look more natural, that is the area where the signal level is high (the red-orange color) becomes smaller, whereas the regions around the TX antenna where the signal level is low become more distinct (marked with the dark blue color). Moreover, if there are more sensors, the position of the TX antenna can be determined with better precision. This effect can be easily noticed when the sizes of the red-orange areas in Fig. 7, 26 sensors and 13 sensors, are compared.

3 Results and discussion

The RMSEs calculated for nearest neighbor, Kriging, and IDW methods with power p from 1 to 6 are shown in Fig. 8.

Figure 8, 13 sensors, presents the results for the scenarios with 13 sensors used for the interpolation process. The differences between the results for individual tests are quite significant. The comparison shows that, irrespectively of the interpolation technique, the RMSE values are smaller for Test_13b than for Test_13a. The RMSE for Test_13b reaches 9.1 dB for IDW p3 and 7.8 dB for Kriging. The RMSE for Test_13a reaches 10.95 dB for IDW p3 and 9.6 for Kriging. The results for NN method are comparable for both tests (RMSE oscillates around 11.85 dB). When Kriging was applied, the RMSE values were the smallest for both compared tests.

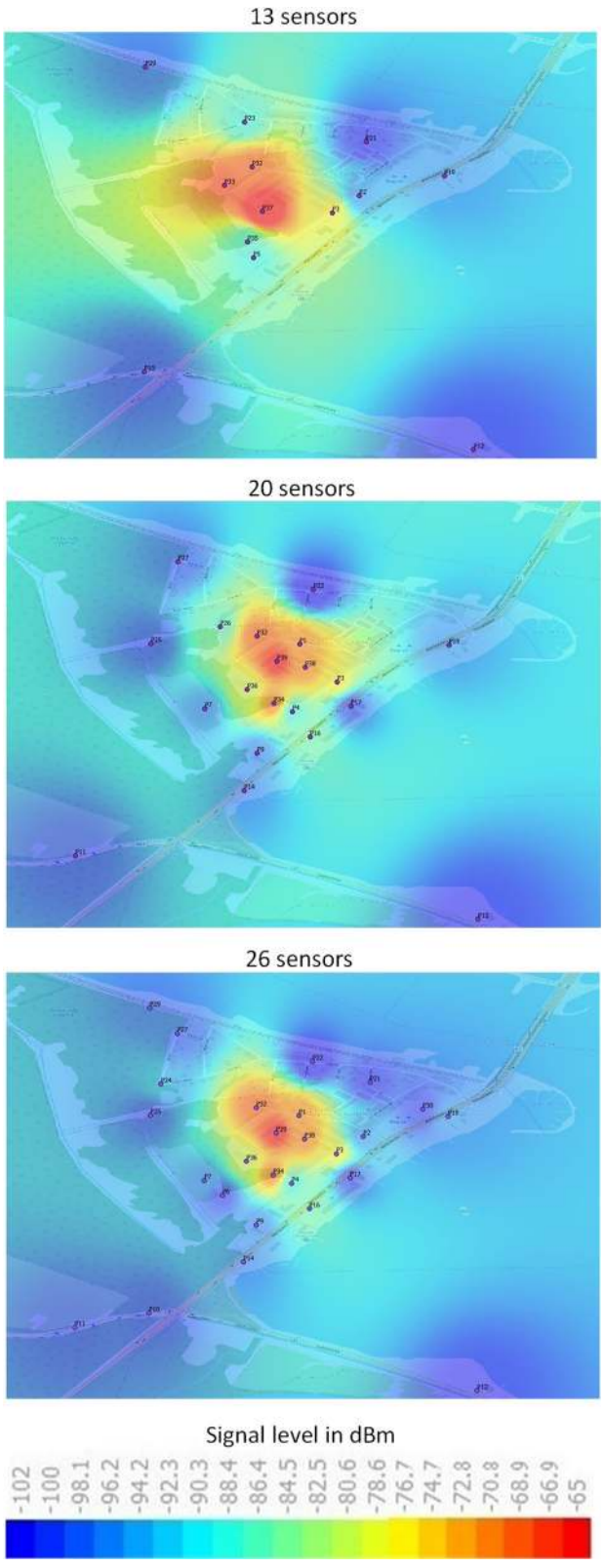

Fig. 6 Maps constructed for IDW p3 interpolation technique. Maps were created for various numbers of sensors

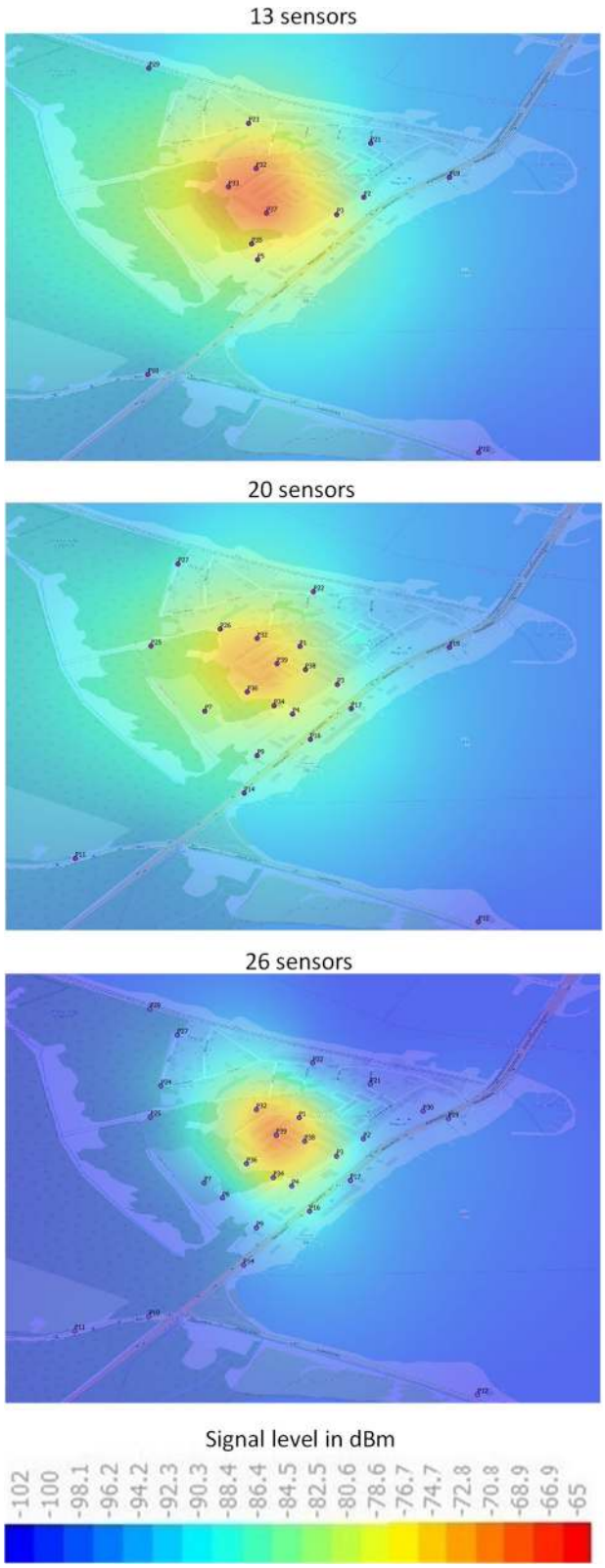

Fig. 7 Maps constructed for Kriging interpolation technique. Maps were created for various numbers of sensors

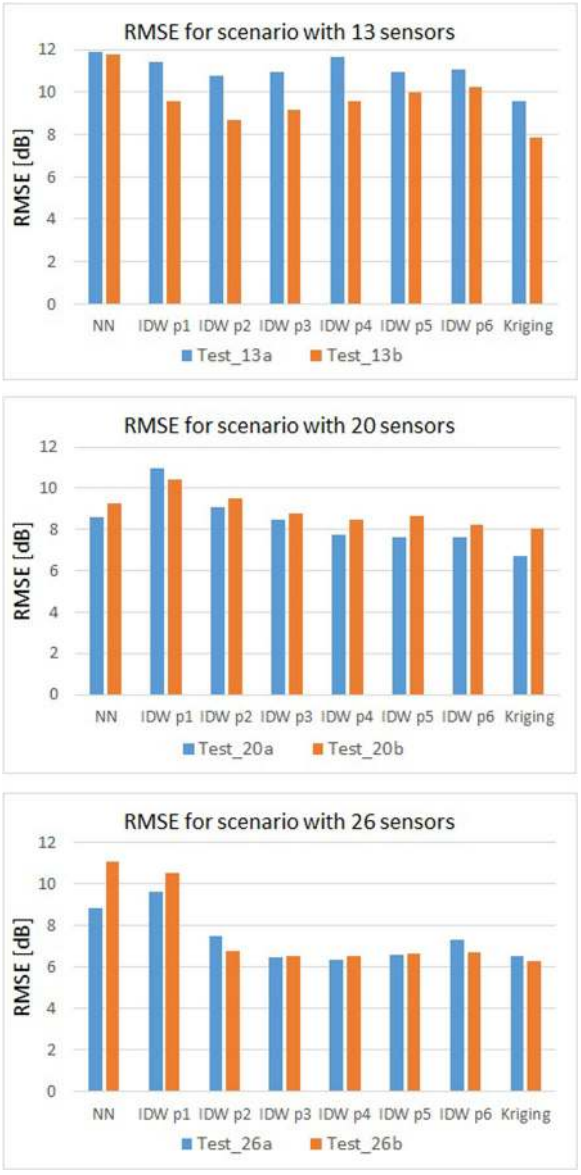

Fig. 8 RMSE for selected interpolation techniques

The results for the scenario with 20 sensors are shown in Fig. 8, 20 sensors. Independently of the applied interpolation technique, the RMSE values are smaller for Test_20a when compared to Test_20b, except the results for IDW p1, which are in fact the worst case (RMSE over 10 dB). The RMSE for Test_20a for IDW p3 reaches 8.5 dB and for Kriging 6.7 dB, while for Test_20b the RMSE reaches 8.8 dB for IDW p3 and 8 dB for Kriging. For both compared tests in this scenario, (1) Kriging offers the best results, and (2) RMSE drops as the power p increases for IDW method. The differences between the results for individual tests are within 1.3 dB.

Figure 8, 26 sensors, presents the results for the scenario with 26 sensors. For both tests the RMSE values are much higher for NN and IDW p1 (between 8.8 dB and 11 dB) than for other interpolation techniques (RMSE from 6.25 to 7.5 dB). In the case of Test_26b, the smallest RMSE occurs for Kriging (6.25 dB), while in the case of Test_

26a, the RMSE reaches the minimum value for IDW p4 (6.3 dB). Unexpectedly, the RMSE for the scenario with 26 sensors for IDW p5 and p6 is higher in comparison to the results for IDW p3 and p4. This observation is valid for both tests in this scenario, i.e., Test_26a and Test_26b.

The average values of RMSE for each scenario are shown in Fig. 9. The effect of the drop in the RMSE as the number of sensors increases is clearly visible for IDW with power p higher than 1 and for Kriging interpolation technique. When IDW p1 method was applied, the benefit of having more sensors in the network was inconsiderable. If NN method was applied, the smallest RMSE value occurred for the scenario with 20 sensors. In general, the trend in the changes of RMSE confirms that placing more sensors in the network makes the quality of REM higher.

In a typical small-scale tactical scenario, troops operate in the area of a few square kilometers and the number of radios that can play the role of sensors amounts to maximum a few dozens. For such conditions (Scenario_20 and Scenario_26), the RMSE in our tests ranged between 6.5 and to 8.5 dB for the IDW p3 and for Kriging. As the measurements were taken in a real environment, the REM quality was assessed to be on a satisfactory level, since the typical fluctuation of the signal level in such conditions is about 5 dB. For the smaller number of sensors (Scenario_13), the quality of REM was lower, as the RMSE reached the level between 8.5 and 10 dB. The characteristic feature of the tactical systems is the fact that neither the number of radios can be increased nor the area of operation can be reduced to get better quality of maps. On the contrary, in civilian systems, such strict limitations do not exist and rearrangement of sensors or placing additional sensors in some areas may be considered an admissible option. The test scenarios reflect the configuration resulting from the organizational structure and the number of devices typically found at the platoon and company level.

4 Conclusions

The quality of maps depends on several factors, among others the density and regularity of deployment of sensors, the distance between sensors, the propagation environment, and the interpolation technique. In this paper, we analyzed the impact of the number of sensors on the REM quality.

In the literature on the subject, mainly scenarios with several hundred measurement points located in the area of around 5 km^2 are studied. In some real applications, this

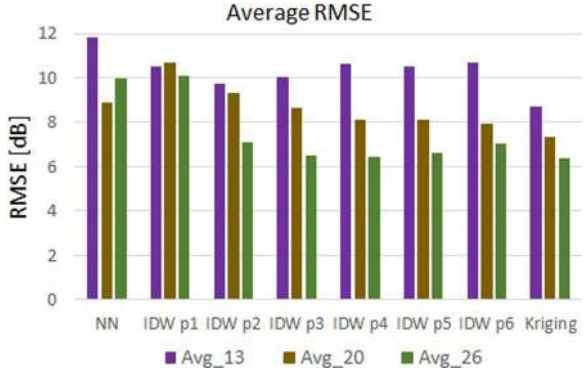

Fig. 9 The average value of RMSE for selected interpolation techniques

number is much lower, e.g., reaching dozens of sensors in the area of approximately 4 km^2. That is why we focused on the scenarios with a small number of sensors that reflect, for example, a small-scale tactical operation or cognitive radio networks operating in suburban areas.

In our research work, we used data from real field tests with 39 sensors deployed within the area of 4 km^2. We analyzed results of the tests with different numbers of sensors (13, 20, and 26) used for the interpolation process. For each scenario, two tests with various arrangements of sensors were analyzed. To create REM maps, the following interpolation techniques were applied: NN, IDW, and Kriging. To assess the quality of maps, the calculated RMSE values were compared. In general, the increase in the number of sensors from 13 to 26 caused a visible improvement in the quality of REM maps. The average RMSE values dropped from 8.7 to 6.3 dB for the Kriging method and from 10 to 6.5 dB for the IDW p3 method.

In the literature on the topic, several methods of interpolation are analyzed. Analyzing our results, the smallest RMSE values were noticed for Kriging and IDW with the power of 3 or 4. For this reason, these interpolation techniques should be recommended for REM construction.

Moreover, we also noticed the influence of the arrangement of sensors on the map quality, which seems to be important in the case of a network with a relatively small number of sensors deployed in a varied terrain. This problem is the subject of another research project conducted by our team.

In general, an increased number of sensors in the network is beneficial, since the RMSE drops significantly. If the number of sensors in the network is limited (for instance, in small tactical operations), the attention should be paid to the optimum deployment of sensors. In the literature on the topic, several methods are presented, although the most promising one seems to be the deployment algorithm based on the stratified approach, which assumes that in some zones the sensor network is more densely covered with sensors than in others.

Our approach to the research was in line with the methodology described above, i.e., some zones were more densely occupied by sensors. A slight difference is that we assume the constant number of sensors for a given scenario and the change of the location of some sensors as the only option possible. Such deployment of sensors seems to be reasonable in diverse areas, like the one presented in this paper, where a slight correction in the arrangement of sensors (Test_a and Test_b) caused a visible change in map quality.

Abbreviations

REM: Radio environment map; MANET: Mobile ad-hoc network; IST: Information systems technology; RTG: Research task group; MCD: Measurement capable device; EW: Electronic warfare; ISR: Intelligence, surveillance, reconnaissance; CR: Cognitive radio; RMSE: Root mean square error; RSS: Received signal strength; RSSD: Received signal strength difference; NN: Nearest neighbor; IDW: Inverse distance weighting

Acknowledgements

The authors thank the anonymous reviewers for their helpful suggestions.

Authors' contributions

All authors have contributed to collecting results, performing analysis, and creating this article. All authors read and approved the final manuscript.

Funding

The article was created as part of the statutory activity of the Military Communications Institute, financed by the Ministry of Science and Higher Education (Poland).

Availability of data and materials
The data collected and analyzed during this study are included in this published article. Any supplementary information is also available from the corresponding author on reasonable request.

Competing interests
The authors declare that they have no competing interests.

Received: 17 December 2019 Accepted: 17 September 2020
Published online: 29 September 2020

References

1. J. Romanik, A. Krasniewski, E. Golan, *RESA-OLSR: RESources-Aware OLSR-based routing mechanism for mobile ad-hoc networks* (International Conference on Military Communications and Information Systems (ICMCIS), Brussels, 2016)
2. J. Romanik, R. Brys, K. Zubel, *Performance analysis of OLSRv2 with ETX, ETT and DAT metrics in static wireless networks* (International Conference on Military Communications and Information Systems (ICMCIS), Warsaw, 2018)
3. M. Malowidzki, P. Kaniewski, R. Matyszkiel, P. Berezinski, *Standard tactical services in a military disruption-tolerant network: field tests* (MILCOM, Baltimore, 2017)
4. M. Suchanski, R. Matyszkiel, P. Kaniewski, M. Kustra, P. Gajewski, J. Lopatka, *Dynamic spectrum management as an anti-interference method. Proceedings of SPIE Vol. 10418* (SPIE, Bellingham, 2017) 2269288, ISSN: 0277-786X, eISSN: 1996-756X (April 20, 2017). DOI: 10.1117/12.2269294
5. M. Suchański, P. Gajewski, J. Łopatka, P. Kaniewski, R. Matyszkiel, M. Kustra, *Coordinated dynamic spectrum management in legacy military communication systems* (WinnComm-Europe 2016 (Wireless Innovation Forum European Conference on Communications Technologies and Software Defined Radio), Paris, 2016)
6. M. Matyszkiel, P. Kaniewski, M. Kustra, J. Jach, *The evolution of transmission security functions in modern military wideband radios. Book Series: Proceedings of SPIE, Volume: 10418, Article Number: UNSP 104180E* (2017)
7. M. Pesko, T. Javornik, A. Košir, M. Štular, M. Mohorčič, *Radio environment maps: the survey of construction methods*, KSII Transactions on Internet and Information Systems, vol 8 (2014), p. 11. https://doi.org/10.3837/tiis.2014.11.008
8. Deliverable D2.4, Final System Architecture, EC FP7-248351 FARAMIR Project, (2011)
9. T. Cai, J. van de Beek, B. Sayrac, S. Grimoud, J. Nasreddine, J. Riihijärvi, P. Mähönen, *Design of layered radio environment maps for RAN optimization in heterogenous LTE systems*, IEEE 22nd International Symposium on Personal, Indoor and Mobile Radio Communications (2011), pp. 172–176. https://doi.org/10.1109/PIMRC.2011.6139803
10. B.H. Yilmaz, T. Tugcu, Location estimation-based radio environment map constructing techniques in fading channels. Wireless Commun. Mobile Comput. **15**(3), 561–570 (2015). https://doi.org/10.1002/wcm.2367
11. M. Suchanski, P. Kaniewski, J. Romanik, E. Golan, *Radio environment maps for military cognitive networks: construction techniques vs. map quality* (International Conference on Military Communications and Information Systems (ICMCIS), Warsaw, 2018). IEEE Xplore). https://doi.org/10.1109/ICMCIS.2018.8398723
12. M. Suchanski, P. Kaniewski, J. Romanik, E. Golan, K. Zubel, *Electronic warfare systems supporting the database of the radio environment maps. Proc. SPIE 11055, XII Conference on Reconnaissance and Electronic Warfare Systems* (2018). https://doi.org/10.1117/12.2524594
13. M. Suchanski, P. Kaniewski, J. Romanik, E. Golan, *Radio environment map to support frequency allocation in military communications systems* (Baltic URSI Symposium, Poznan, 2018)
14. Ezzati, N., Taheri, H., Tugcu, T.: Optimised sensor network for transmiter localisation and radio environment mapping. The Institution of Engineering and Technology, IET Communications, pp. 2170–2178, 10(16) (2016). DOI: https://doi.org/10.1049/iet-com.2016.0341.
15. M. Patino, F. Vega, *Model for measurement of radio environment maps and location of white spaces for cognitive radio deployment*, IEEE-APS Topical Conference on Antennas and Propagation in Wireless Communications (2018). https://doi.org/10.1109/APWC.2018.8503755
16. D. Mao, W. Shao, Z. Qian, H. Xue, X. Lu, H. Wu, *Constructing accurate radio environment maps with Kriging interpolation in cognitive radio networks*, (CSQRWC2018) Cross Strait Quad-Regional Radio Science and Wireless Technology Conference (2018). https://doi.org/10.1109/CSQRWC.2018.8455448
17. S. Alfattani, A. Yongacoglu, *Indirect methods for constructing radio environment Map*, (CCECE) IEEE Canadian Conference on Electrical & Computer Engineering (2018). https://doi.org/10.1109/CCECE.2018.8447654
18. F. Frantzis, V.-P. Chowdappa, C. Botella, J.J. Samper, R.J. Martinez, *Radio environment map estimation based on communication cost modeling for heterogeneous networks* (IEEE 85th Vehicular Technology Conference (VTC Spring), Sydney, 2017). https://doi.org/10.1109/VTCSpring.2017.8108227
19. A. Kliks, P. Kryszkiewicz, K. Cichoń, A. Umbert, J. Pérez-Romero, F. Casadevall, *DVB-T channels power measurements in in-door/outdoor cases* (IEICE Information and Communication Technology Forum, Poznan, 2014)
20. Yilmaz, H. B., Tugcu, T., Alagöz, F., and Bayhan, S.: Radio environment map as enabler for practical cognitive radio networks. In: IEEE Communications Magazine, 162-169, 51(12) (2013). DOI: https://doi.org/10.1109/MCOM.2013.6685772.
21. S. Roger, C. Botella, J.J. Perez-Solano, J. Perez. Application of radio environment map reconstruction techniques to platoon-based cellular V2X communications. Sensors. **20**, 2440 (2020). https://doi.org/10.3390/s20092440
22. A. Kliks, P. Kryszkiewicz, Ł. Kułacz, *Measurement-based coverage maps for indoor REMs operating in TV band*, IEEE International Symposium on Broadband Multimedia Systems and Broadcasting (2017). https://doi.org/10.1109/BMSB.2017.7986162
23. J. Ojaniemi, J. Kalliovaara, J. Poikonen, R. Wichman, *A practical method for combining multivariate data in radio environment mapping*, IEEE 24th Annual International Symposium on Personal, Indoor, and Mobile Radio Communications (2013). https://doi.org/10.1109/PIMRC.2013.6666232

Publisher's Note